

Received March 1, 2019, accepted March 18, 2019, date of publication March 22, 2019, date of current version April 8, 2019.

Digital Object Identifier 10.1109/ACCESS.2019.2906980

# Improved Kidney-Inspired Algorithm Approach for Tuning of PID Controller in AVR System

SERDAR EKİNCİ<sup>1</sup> AND BARAN HEKİMOĞLU<sup>2</sup>, (Member, IEEE)

<sup>1</sup>Computer Engineering Department, Batman University, 72100 Batman, Turkey

<sup>2</sup>Electrical and Electronics Engineering Department, Batman University, 72100 Batman, Turkey

Corresponding author: Baran Hekimoğlu (baran.hekimoglu@batman.edu.tr)

**ABSTRACT** This paper proposes a novel tuning design of proportional integral derivative (PID) controller via an improved kidney-inspired algorithm (IKA) with a new objective function. The main objective of the proposed approach is to optimize the transient response of the AVR system by minimizing the maximum overshoot, settling time, rise time and peak time values of the terminal voltage, and eliminating the steady state error. After obtaining the optimal values of the three gains of the PID controller ( $K_P$ ,  $K_I$ , and  $K_D$ ) with the proposed approach, the transient response analysis was performed and compared with some of the current heuristic algorithms-based approaches in literature to show the superiority of the optimized PID controller. In order to evaluate the stability of the automatic voltage regulator (AVR) system tuned by IKA method, the pole/zero map analysis and Bode analysis are performed. Finally, the robustness analysis of the proposed approach has been carried out with variations in the parameters of the AVR system. The numerical simulation results demonstrated that the proposed IKA tuned PID controller has better control performances compared to the other existing approaches. The essence of the presented study points out that the proposed approach may successfully be applied for the AVR system.

**INDEX TERMS** Automatic voltage regulator, improved kidney-inspired algorithm, PID tuning, robustness analysis, transient response.

## I. INTRODUCTION

### A. RESEARCH BACKGROUND

Automatic voltage regulator (AVR) is essential equipment that is used in power system utilities. As its name implies, the main objective of AVR is to control the terminal voltage of synchronous generator by adjusting its exciter voltage. Due to the high inductance of the generator field windings and load variations, stable and fast response of the regulator is difficult to achieve [1]. Therefore, it is important to improve the AVR performance and ensure stable and efficient response to transient changes in terminal voltage. So far, different control techniques have been proposed by researchers to analyze the AVR system with an aim to gain better dynamic response. However, among these controllers the classical proportional plus integral plus derivative (PID) is the most preferable controller because of its simple design structure and robustness to variations of the system parameters [2].

### B. LITERATURE SURVEY

The optimal tuning of the gain parameters ( $K_P$ ,  $K_I$  and  $K_D$ ) of the PID controller is a very difficult problem.

The associate editor coordinating the review of this manuscript and approving it for publication was Fangfei Li.

These gain parameters can be calculated by either trial-and-error or traditional methods such as Ziegler-Nichols (ZN) and Cohen-Coon (CC) [3], [4]. Trial-and-error takes quite some time and in most cases does not yield optimal results. In ZN and CC methods, the controller parameters are obtained for an operating point where the model can be evaluated linearly. However, these two methods do not find the optimal PID parameters and generate undesirable overshoots and long-term oscillations in the system. In addition, these two methods contain a large number of mathematical calculations that make it difficult to find optimal PID controller parameters. On the other hand, artificial intelligence approaches such as fuzzy logic and neural network were applied to solve the optimization problem of PID controller parameters [5], [6]. However, the training process and the duration of convergence time become weighty and long in the artificial neural network. As for a fuzzy logic system, successful generation of fuzzy membership functions generally depend on the analysis of data, tuning of a model and skills of the designer [6], [7]. In recent years, evolutionary-based many heuristic optimization algorithms have been proposed for the setting of PID controller parameters in the AVR system, rather than using the fore-mentioned traditional tuning methods that fail to operate

effectively under different operating conditions and that perform poorly. Recently, heuristic optimization based tuning methods like bio-geography-based optimization (BBO) [8], gravitational search algorithm (GSA) [9], [10], grasshopper optimization algorithm (GOA) [11], continuous firefly algorithm (CFA) [12], local unimodal sampling (LUS) algorithm [13], teaching learning-based optimization (TLBO) [14], Taguchi combined genetic algorithm (TCGA) [15], many optimizing liaisons (MOL) algorithm [16], anarchic society optimization (ASO) [17], pattern search algorithm (PSA) [18], differential evolution (DE) [19], artificial bee colony (ABC) [19], chaotic optimization based on Lozi map (COLM) [20], chaotic ant swarm (CAS) [21], particle swarm optimization (PSO) [22], stochastic fractal search (SFS) algorithm [23], symbiotic organisms search (SOS) algorithm [24], bacterial foraging optimization algorithm (BFOA) [25], ant lion optimizer (ALO) [26], sine cosine algorithm (SCA) [27], salp swarm algorithm (SSA) [28], world cup optimization (WCO) [29], monarch butterfly optimization (MBO) algorithm [30] and cuckoo search (CS) [6] have been applied for optimal tuning of PID controller of an AVR system.

In the literature, the most studied heuristic optimization based tuning methods proposed for the AVR system are PSO, GA, ABC and DE. Besides, the ZN tuning method is the only classical method used for the very same system. A concise literature survey of the tuning methods used for the AVR system over the last decade is given in Table 1. This table also summarizes the performance indices and analysis methods used so far.

### C. MOTIVATION FOR THE PRESENT WORK

As can be seen from the literature survey in Table 1, heuristic algorithms were preferred for the optimization of PID controller in the AVR system. In all studies given in the table, the aim is to improve the system response by reducing the transient response parameters such as maximum overshoot percentage ( $M_p\%$ ), settling time ( $t_s$ ), rise time ( $t_r$ ), peak time ( $t_p$ ), and steady state error ( $E_{ss}$ ). To achieve this, it is essential to obtain the best PID controller gains. However, due to the lack of the proposed algorithms to improve the performance of the AVR system, they do not find the optimal gains of the PID controller. For example, although GA, PSO and ABC have great potential to solve many optimization problems, they suffer from memory capability and computational burden. Better results may be achieved with other optimization approaches. However, these algorithms have disadvantages such as local minimum stagnation, early convergence, difficulty in the selection of control parameters and increased calculation time depending on the size of the system studied [31], [32]. In addition, there is no precise algorithm for the best solution of the PID controller parameters in the AVR system. Therefore, studying a new heuristic optimization algorithm is an important and observable problem for researchers.

In addition to the deficiencies of optimization algorithms, the selected objective function also significantly affects the performance of the AVR system. From Table 1, the classical integral-based objective functions used in the literature are integrated squared error (ISE), integrated absolute error (IAE), integrated time multiplied absolute error (ITAE), and integrated time multiplied squared error (ITSE). In addition, the objective function proposed by Zwe-Lee Gaing (ZLG) [22] uses a combination of transient response criteria containing  $M_p\%$ ,  $E_{ss}$ ,  $t_s$  and  $t_r$ . In AVR studies, the optimization is performed by especially using the objective functions, ITSE and ZLG. However, in studies using the ITSE objective function [11], [19], [23] the  $M_p\%$  value is quite high, whereas in studies using the ZLG objective function [12], [22], [27] especially the  $t_p$  ve  $t_r$  values are very high. These deficiencies can be overcome by using a new objective function that consist ITSE and ZLG objective functions together with an appropriate weighting factor, so that all the transient response parameters will be reasonable.

The kidney-inspired algorithm (KA), a powerful and efficient global optimization technique, was proposed by Jaddi et al. in 2017 [33]. This algorithm is inspired by four functions (filtering, reabsorbing, secreting and excreting) in the physiological structure of the kidney urinary system. Preliminary studies have shown that the optimizing capability of KA is superior to other optimization algorithms such as PSO and GA and those used in unconstrained optimization problems [33]. The compatible balance between exploration and exploitation stages is the most important feature of this algorithm and thus has a better convergence characteristic. Since it is a new algorithm, several research subjects have not been implemented yet except for a few engineering applications [34]–[37]. In addition to that further improvement has been made to the original algorithm to make it a self-adaptive algorithm, which does not require parameter tuning in advance and to enhance its convergence ability without compromising the balance between exploration and exploitation stages [38]. This improved algorithm can increase the accuracy of the solution to some extent in a reasonable time, in which the original KA cannot do on its own. Hence, the IKA technique not only has a high level of exploration capability, which leads to explore the potential regions of the search space but also has a high exploitation capability, which assists the IKA technique to rapidly converge towards the optimum and exploit it accurately. Considering these superior features and advantages of IKA technique, in this study, an IKA-based PID (IKA-PID) controller was proposed for high-order AVR system in order to minimize the  $M_p\%$ ,  $t_s$ ,  $t_r$  and  $t_p$  values of the synchronous generator terminal voltage and to eliminate the steady state error in the system.

### D. CONTRIBUTION OF THE PRESENT WORK

The outstanding contributions of this study can be summarized as follows:

**TABLE 1.** The tuning methods used for AVR system in literature.

Reference			[8]	[9]	[11]	[10]	[12]	[13]	[14]	[15]	[16]	[17]	[18]	[19]	[20]	[21]	[22]	[23]	[24]	[25]	[26]	[27]	[28]	[29]	[30]	[6]	
Tuning methods	Classical	ZN			◇																	◇	◇				
	Heuristic optimization	ABC	◇	◇	◇			◇			◇		◇	◆				◇	◇	◇	◇	◇	◇			◇	
		ALO																			◆						
		ASO											◆														
		BBO	◆																◇	◇			◇				
		BFOA																			◆	◇				◇	
		CAS														◆					◇				◇		
		COLM														◆									◇		
		CPSO															◆								◇		
		CS																				◇				◆	
		DE	◇	◇	◇			◇				◇			◇						◇	◇	◇				
		CFA					◆																				
		GA				◇				◇							◇	◇				◇				◇	
		GOA			◆																						
		GSA		◆		◆													◇								
		GWO																				◇					
		ICA																						◇			
		KA																									
		LUS						◆											◇	◇						◇	
		MBO																							◆		
		MOL										◆							◇		◇	◇				◇	◇
		PSA												◆													
		PSO	◇	◇		◇	◇	◇		◇	◇	◇			◆				◆		◇	◇			◇	◇	◇
		SCA																					◆				
		SFS																		◆							
		SOS																			◆						
		SSA																						◆			
		TCGA										◆															
		TLBO								◆																	◇
	WCO																		◇					◆			
Performance indices	IAE		◆				◆			◆											◆				◆		
	ISE		◆				◆			◆											◆				◆		
	ITAE		◆			◆	◆	◆		◆	◆				◆						◆			◆	◆		
	ITSE	◆	◆	◆			◆			◆			◆					◆			◆		◆				
	ZLG		◆			◆											◆			◆		◆					
	Other				◆					◆		◆	◆			◆	◆			◆						◆	
Analysis methods	Transient	◆	◆	◆	◆	◆	◆	◆	◆	◆	◆	◆	◆	◆	◆	◆	◆	◆	◆	◆	◆	◆	◆	◆	◆	◆	
	Pole/zero map	◆					◆			◆		◆	◆	◆				◆	◆	◆	◆	◆	◆				
	Bode	◆					◆			◆		◆	◆	◆				◆	◆	◆	◆	◆			◆		
	Robustness	◆	◆	◆			◆	◆		◆	◆	◆	◆	◆	◆	◆		◆	◆	◆	◆	◆		◆		◆	

◆ Proposed method

◇ Method used for comparison with the proposed method

- 1) The IKA technique and a new objective function have been proposed for the first time in the PID controller design of the AVR system. This constitutes the most important originality of the study.
- 2) The values of  $M_p\%$ ,  $t_s$ ,  $t_r$  and  $t_p$  obtained by IKA and the values of ITSE and ZLG objective functions were compared with those obtained by other optimization algorithms published in the literature (PSO [39], DE [19], ABC [19], LUS [13], PSA [18], BBO [8], and

GOA [11]). The results clearly show the effectiveness of the proposed approach.

- 3) The stability performance of the proposed IKA-PID controller was investigated by performing transient response, pole/zero map and Bode analysis.
- 4) In addition, the robustness of the PID controller tuned by IKA under the parameter changes of the AVR system was investigated.

## II. LINEARIZED AVR SYSTEM MODEL USING PID CONTROLLER

### A. DESCRIPTION OF THE LINEARIZED AVR SYSTEM

The role of an AVR is to maintain a synchronous generator's terminal voltage magnitude at a predefined level to enhance the power system stability and quality via the generator exciter control. Fig. 1 illustrates a typical arrangement of a simple AVR system. From the figure, it can be seen that there are four essential components that constitute an AVR system; amplifier, exciter, generator, and sensor [40]. Thus, the transfer function of the AVR system can be modeled through the linearized transfer function of each component as follows:

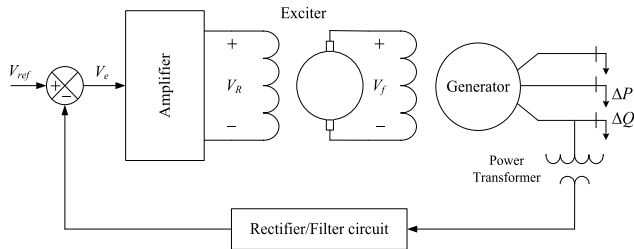


FIGURE 1. A typical arrangement of a simple AVR.

The amplifier model is given by the following transfer function [40]:

$$G_{\text{Amplifier}}(s) = \frac{K_A}{1 + sT_A} \quad (1)$$

where  $K_A$  is the amplifier gain and  $T_A$  is the amplifier time constant. The typical values are in the range of 10 – 40 and 0.02 – 0.1 s, and the used values in this paper are 10 and 0.1 s, respectively.

The exciter model is given by the following transfer function [40]:

$$G_{\text{Exciter}}(s) = \frac{K_E}{1 + sT_E} \quad (2)$$

where  $K_E$  is the exciter gain and  $T_E$  is the exciter time constant. The typical values are in the range of 1.0 – 10 and 0.4 – 1.0 s, and the used values in this paper are 1.0 and 0.4 s, respectively.

The load dependent generator model is given by the following transfer function [40]:

$$G_{\text{Generator}}(s) = \frac{K_G}{1 + sT_G} \quad (3)$$

where  $K_G$  is the generator gain and  $T_G$  is the generator time constant. The typical values are in the range of 0.7 – 1.0 and 1.0 – 2.0 s. In this paper, for the nominal operating conditions, these values are taken as 1.00 and 1.00, respectively.

Finally, the sensor model is given by the following transfer function [40]:

$$G_{\text{Sensor}}(s) = \frac{K_S}{1 + sT_S} \quad (4)$$

where  $K_S$  is the sensor gain and  $T_S$  is the sensor time constant. The typical values are in the range of 1.0 – 2.0 and 0.001 – 0.06 s, and the used values in this paper are 1.0 and 0.01 s, respectively.

When all of these linearized transfer function of AVR components are used, the following linearized transfer function of AVR system without PID controller is obtained:

$$\frac{\Delta V_t(s)}{\Delta V_{ref}(s)} = \frac{K_A K_E K_G (1 + sT_S)}{(1 + sT_A)(1 + sT_E)(1 + sT_G)(1 + sT_S) + K_A K_E K_G K_S} \quad (5)$$

Using the fore-mentioned values of system parameters, the step voltage response of AVR system without controller is obtained as shown in Fig. 2.

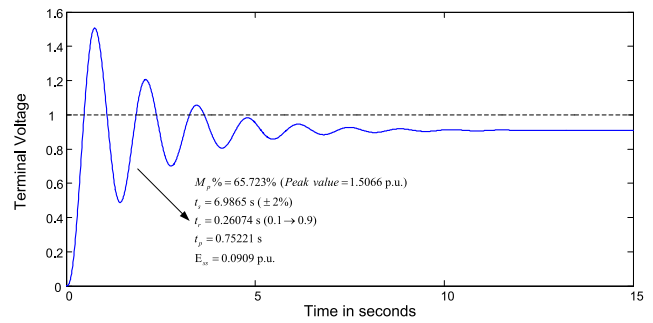


FIGURE 2. Output voltage step response of AVR system in the absence of controller.

From the figure, it is clear that despite being stable, the step voltage response is highly oscillatory and has a steady state error. The system has two complex poles at  $s = -0.5198 \pm 4.6642i$  with a damping ratio of 0.111 and two real poles at  $s = -99.971$  and  $s = -12.489$ . The rise time of the system is 0.261 s, the peak time is 0.752 s, the settling time is 6.99 s, the overshoot is 65.7% and the steady state value is 0.909 p.u., thus a steady state error of 0.091 p.u. It is obvious that the dynamic response of the AVR system needs to be improved and the steady state error should be eliminated by using a PID controller.

### B. ESSENTIALS OF PID CONTROLLER

PID controller is the most preferred controller type in industry due to its reliable and simple structure, and yields a robust performance over a wide range of operating conditions when its parameters tuned properly and jointly [3], [11]. The s-domain transfer function of PID controller is given as follows [3]:

$$G_{PID}(s) = \frac{U(s)}{E(s)} = K_P + \frac{K_I}{s} + K_D s \quad (6)$$

where  $U(s)$  is the actuating control signal working on the error signal  $E(s)$ , which is the difference between the reference and the measured values of the process output,  $K_P$  is the proportional gain,  $K_I$  is the integral gain, and  $K_D$  is the derivative gain.

### C. ANALYSIS OF THE AVR SYSTEM WITH PID CONTROLLER

The block diagram of AVR system with PID controller is illustrated in Fig. 3. The transfer function of AVR system with PID controller is given as (7), shown at the bottom of this page.

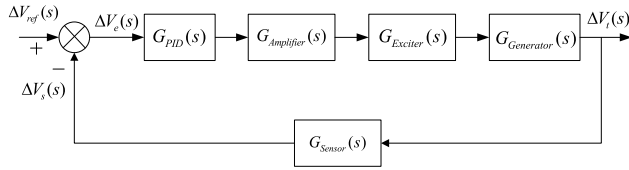


FIGURE 3. AVR system with PID controller.

PID controller tuning can be done by the ZN method which is one of the classical techniques. The PID gains obtained by the ZN method at nominal operating condition ( $K_G = 1.00$  ve  $T_G = 1.00$  s) of AVR system are  $K_P = 1.0210$ ,  $K_I = 1.8743$  and  $K_D = 0.1390$ . Fig. 4 illustrates the response of the AVR system terminal voltage for a unity step input. From the figure, it can be seen that the AVR system with its PID controller tuned by the ZN method is highly oscillatory ( $M_p\% = 51.495$ ) and the settling time ( $t_s = 3.0516$  s) is quite long. As can be seen from the figure, since the PID tuning with the classical tuning method does not provide the desired performance, the IKA technique, which is a recently proposed effective heuristic algorithm, is used for designing the PID controller in AVR system, in this study.

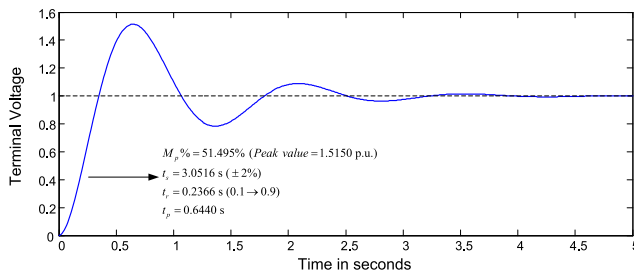


FIGURE 4. Output voltage step response of AVR system with ZN-based controller.

## III. OVERVIEW OF KA AND IKA

### A. KA

Kidneys are very important organs in the urinary system of the human biological structure that have vital functions such as filtering the blood by elimination of excessive water and wastes via urine and handling the amounts of ions in the blood. Hence, they are responsible for blood chemistry, fluid balance and so the general state of health of the human body. The kidney process is a repeated process that can be

summarized by four stages: filtration, reabsorption, secretion, and excretion. The filtration starts in the glomerular capillaries where dissolved substances are transferred into the tubules under the pressure of both Bowman's capsule and blood. Then the reabsorption is performed in order to return the useful substances in solutes from the tubules to the bloodstream. The secretion is the movement of the solutes towards the renal tubule thereafter the excessive substances (water, wastes and ions) in the urine is excreted. Fig. 5 illustrates the basic physiological mechanism of the kidney.

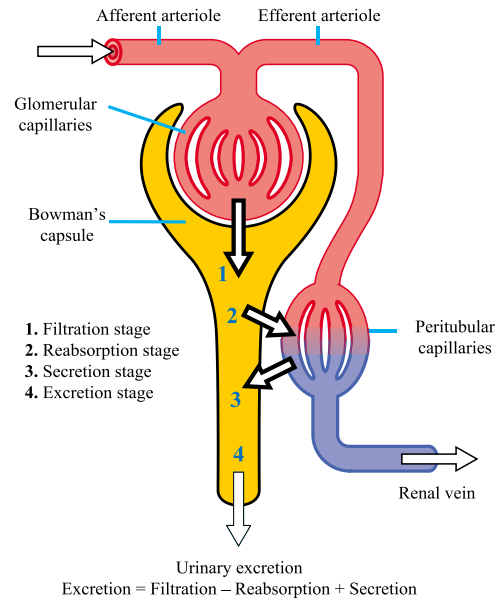


FIGURE 5. Biological kidney system [41].

The kidney-inspired algorithm (KA), which simulates the fore-mentioned functions of the kidneys in the human body, was proposed by Jaddi et al. (2017) [33]. In the initial stage of the KA an arbitrary populace of possible solutes is generated as in other population-based algorithms and their objective functions are computed. Each solute can be considered as particles of water and solutes in plasma in the biological kidney system. In each iteration, a new solute is created for all solutes by moving towards the best solute obtained so far. The movement of a solute in this algorithm is formulated as follows [31], [33]:

$$S_{i+1} = S_i + rand(S_{best} - S_i) \quad (8)$$

where  $S$  is a solute in the population,  $S_i$  is a solute in the  $i$ th iteration,  $rand$  is a random number between zero and a given number, and  $S_{best}$  is the best solute obtained so far in previous iterations. By applying the filtration operator, the solutes in the populace with higher quality are filtered

$$\frac{\Delta V_t(s)}{\Delta V_{ref}(s)} = \frac{K_A K_E K_G (1 + sT_S)(s^2 K_D + sK_P + K_I)}{s(1 + sT_A)(1 + sT_E)(1 + sT_G)(1 + sT_S) + K_A K_E K_G K_S (s^2 K_D + sK_P + K_I)} \quad (7)$$



into the filtered blood (FB) and the remaining solutes are moved into the waste (W). For this purpose, a filtration rate that is calculated and updated in each iteration is used in the KA. The filtration rate ( $fr$ ) is analog to glomerular filtration rate in the biological kidney system and is calculated as follows [31], [33]:

$$fr = \alpha \times \sum_{i=1}^p f(x_i)/p \quad (9)$$

where  $\alpha$  is a constant value in a range of [0,1],  $f(x_i)$  is the objective function of solute  $x$  at  $i$ th iteration,  $p$  is the population size. The rule to be followed in order to determine whether to accept a solute as a member of FB or W is such that; if the quality of the solute is greater than  $fr$ , it is accepted as a member of FB, otherwise, it is accepted as a member of W. If a solute is placed to W, the reabsorption operator provides it another chance to improve itself to become a portion of FB. This can only happen if it satisfies the filtration rate after applying the movement operator in (8) again. This is analog to the reabsorption of the useful particles into the bloodstream in the biological kidney system. If this chance is not satisfied, the solute is excreted from W and another random solute is inserted into W instead. Moreover, if, after the filtration operation, a solute that is placed to FB is better than the worst solute in FB, then the worst solute is secreted (removed) from FB. However, if that solute is not better than the worst solute in FB, then it is secreted. This is analog to the secretion of the harmful particles from bloodstream in the biological kidney system. After that, the solutes in FB are ranked in order to update the best solute obtained so far. Finally, FB and W are merged to form a new population and the filtration rate is updated. When the termination criterion is reached, this repeated process comes to an end. The addition of random solutes can be considered as the continuous addition of water and solutes into the glomerular capillaries in the biological kidney system.

## B. IMPROVED KA (IKA)

Since the major goal of all optimization algorithms is to find the global optimum solution, it is very important to achieve a balance between the exploration (global search) and the exploitation (local search) phases of the algorithm. Therefore, in order to achieve this goal, the basic algorithm will be improved through two modifications, both of which are proposed by Jaddi et al. [38]. In this paper, the modified algorithm is called improved KA (IKA).

### 1) CONTROLLING THE FILTRATION RATE

The first modification applied to the basic algorithm is to control the filtration rate during the search process. Since the convergence rate of the basic KA is tuned by the value of  $\alpha$  in the filtration rate, which is set to a fixed value in advance, changing it dynamically to a fine-tuned value in each iteration will extent the performance of the algorithm significantly. If the value of  $\alpha$  is large, more solutes will

move to W and this will cause more exploitation of the search space. In contrast, if the value of  $\alpha$  is small, more solutes will move to FB and this will cause more exploration of the search space. When there is high exploitation there may not be enough solutes in FB to perform enough exploration. This may lead to local optima stagnation and therefore degrade the algorithm's performance. Thus, it is clearly important to fine-tune  $\alpha$  appropriately so that it does not affect the algorithm's convergence ability. At the beginning of the search process, the value of  $\alpha$  must be small enough for an effective exploration of the search space. In later iterations, it has to be increased to slowly increase the exploitation of the search space in order to accelerate the algorithm's convergence. In the proposed IKA,  $\alpha$  is set to zero initially, which is the minimum value and then it is slowly increased with a rate that is given in (10) in each iteration until it reaches the maximum value of 1 [38]:

$$IR_i^\alpha = 1 - \frac{iteration_i}{num\_ite} \quad (10)$$

where  $IR_i^\alpha$  represents the increasing rate in the  $i$ th iteration,  $iteration_i$  is the number of the current iteration, and  $num\_ite$  represents the total number of iterations. The dynamic change of the filtration rate not only reduces the number of parameters in the algorithm but also balances the exploration and exploitation phases during the search process.

### 2) USE OF CHAOTIC LOGISTIC MAP

The use of a chaotic map, namely logistic map, is the second modification that is realized to further improve the convergence speed of the algorithm while keeping the balance between the exploration and exploitation phases. The logistic map is used to generate a chaotic sequence instead of using a random number in the movement formula (8) of the IKA. This type of map is a form of polynomial mapping and is given mathematically as follows [38]:

$$y_{k+1} = r \cdot y_k \cdot (1 - y_n) \quad (11)$$

where the  $y$  is a variable and for  $k = 1, 2, 3, \dots, y_k$  and  $y_{k+1}$  are the  $k$ th and  $(k+1)$ th values of  $y$ , respectively. Here,  $r = 4$ , so that a range of [0,1] can be achieved.

For more detailed information and processing steps on KA and IKA algorithms, please refer to [33] and [38], respectively.

## IV. MATHEMATICAL PROBLEM FORMULATION

The design steps of the proposed IKA-based PID controller is presented in this section.

### A. DESIGN OF THE PROPOSED OBJECTIVE FUNCTION

The performance of the AVR system is evaluated by taking into account the maximum overshoot percentage ( $M_p\%$ ), settling time ( $t_s$ ), rise time ( $t_r$ ), peak time ( $t_p$ ), and steady state error ( $E_{ss}$ ) values from the time domain criteria. When the values of  $M_p\%$ ,  $t_s$ ,  $t_r$ ,  $t_p$  and  $E_{ss}$  of the step response are minimum, the system will have the best performance. In literature,

the most preferred objective functions for the AVR system are ITSE and ZLG and are defined as follows [11], [42]:

$$ITSE = \int_0^{t_{sim}} t \cdot e^2(t) \cdot dt \quad (12)$$

$$ZLG = (1 - e^{-\beta}) \cdot (M_p + E_{ss}) + e^{-\beta}(t_s - t_r) \quad (13)$$

where  $t_{sim}$  is the simulation duration,  $e(t) = V_{ref} - V_s(t)$  is the error signal and  $\beta$  is a weighting factor in the range of [0.5,1.5]. Although the ITSE and ZLG objective functions improve the transient response of the AVR system, the detailed and rigorous research has showed that in studies using ITSE [11], [19], [23],  $M_p\%$  were high, whereas in studies using ZLG [12], [22], [27],  $t_r$  and  $t_p$  times were high. In order to overcome these disadvantages, a new performance criterion based on the combination of the two objective functions has been designed for the first time in this paper and is defined as follows:

$$J(\bar{K}) = \mu \cdot ITSE + ZLG \quad (14)$$

where  $J(K'') = [K_P, K_I, K_D]$ ;  $\mu$  is the weight factor that regulates the balance between ITSE and ZLG. If  $\mu$  increase,  $M_p\%$  will increase and if  $\mu$  decrease  $t_r$  and  $t_p$  will increase. During the iterative simulations, this parameter is found to be between 30 and 70 and its best value is 50.

### B. CONSTRAINTS OF THE PRESENT WORK

Determining the lower and upper limits of the gains in PID controller tuning is important. Therefore the limits to be used in the optimization problem are defined as follows:

$$\begin{aligned} K_P^{\min} &\leq K_P \leq K_P^{\max} \\ K_I^{\min} &\leq K_I \leq K_I^{\max} \\ K_D^{\min} &\leq K_D \leq K_D^{\max} \end{aligned} \quad (15)$$

where *min* and *max* superscripts refers to minimum and maximum values of the controller parameters, respectively. In order to make an appropriate comparison with other studies in the literature and to find the optimal values of PID gains, the range of gains is taken as [0.2, 2.0], in this study.

### C. IMPLEMENTATION OF THE PROPOSED IKA-PID CONTROLLER IN AVR SYSTEM

In order to improve the transient response of the AVR system in terms of  $M_p\%$ ,  $t_s$ ,  $t_r$ ,  $t_p$  and  $E_{ss}$  criteria, the best values of the PID controller parameters can be found using the IKA technique, which is relatively new and has excellent global and local exploration capabilities. The block diagram of the AVR system with the recommended IKA tuned PID controller is shown in Fig. 6.

In order to optimize the three PID controller parameters by using IKA algorithm, the design parameters are first coded to a solute, such as  $P = [K_P; K_I; K_D]$ , where each solute represented by a real number. The solutes are then optimized by following the basic steps of the IKA technique to minimize

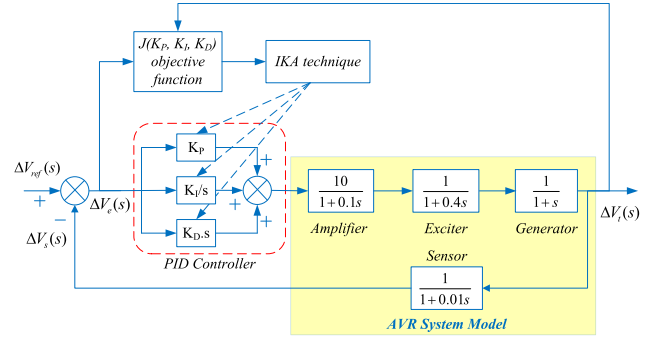


FIGURE 6. AVR system with IKA-based PID controller.

the value of an objective function. In the proposed approach, the first population contains randomly selected  $m$  number of solutes (population size). For each solute, the AVR system is simulated in the time domain and the voltage variation curves are obtained. Each solute is likely to give a different voltage response curve with corresponding  $M_p\%$ ,  $t_s$ ,  $t_r$ ,  $t_p$  and  $E_{ss}$  values. Then the objective function values of each solute according to (14) are determined and the solutes are returned to the optimization module for subsequent iteration. This bidirectional movement between the AVR system and the optimization module is repeated up to a specified termination condition (maximum number of iterations). After the end of the optimization process, the best solute having the lowest value of the objective function in (14) is recognized as the optimal PID parameter set. A detailed flow diagram of the IKA technique applied to optimize the performance of the AVR system is shown in Fig. 7.

### V. SIMULATION RESULTS AND DISCUSSIONS

All simulations and IKA technique encodings were made using the MATLAB/Simulink program (Version 8.3) on an Intel i7 2.50 GHz processor with a 16.00 GB RAM computer. The maximum number of iterations for IKA is chosen as 40 and the maximum population (solute) number is chosen as 30. The best results in the related tables are highlighted in bold font. The important results of this study are shown in the following subsections.

#### A. CONVERGENCE PROFILE

The minimum  $J(\bar{K})$  in each iteration is recorded to obtain the convergence characteristic of the proposed IKA technique for AVR. Fig. 8 shows the IKA-based convergence profile of the optimization process. As can be seen from the figure, the proposed objective function  $J(\bar{K})$  converges to the global optimum value in only 7 iterations, which is quite fast.

The IKA-PID controller parameters obtained at the end of the optimization process shown in Fig. 7 are  $K_P = 1.0426$ ,  $K_I = 1.0093$  and  $K_D = 0.5999$ . The transfer function obtained according to these parameters is given in (16). Fig. 9 shows the AVR terminal voltage step response of the

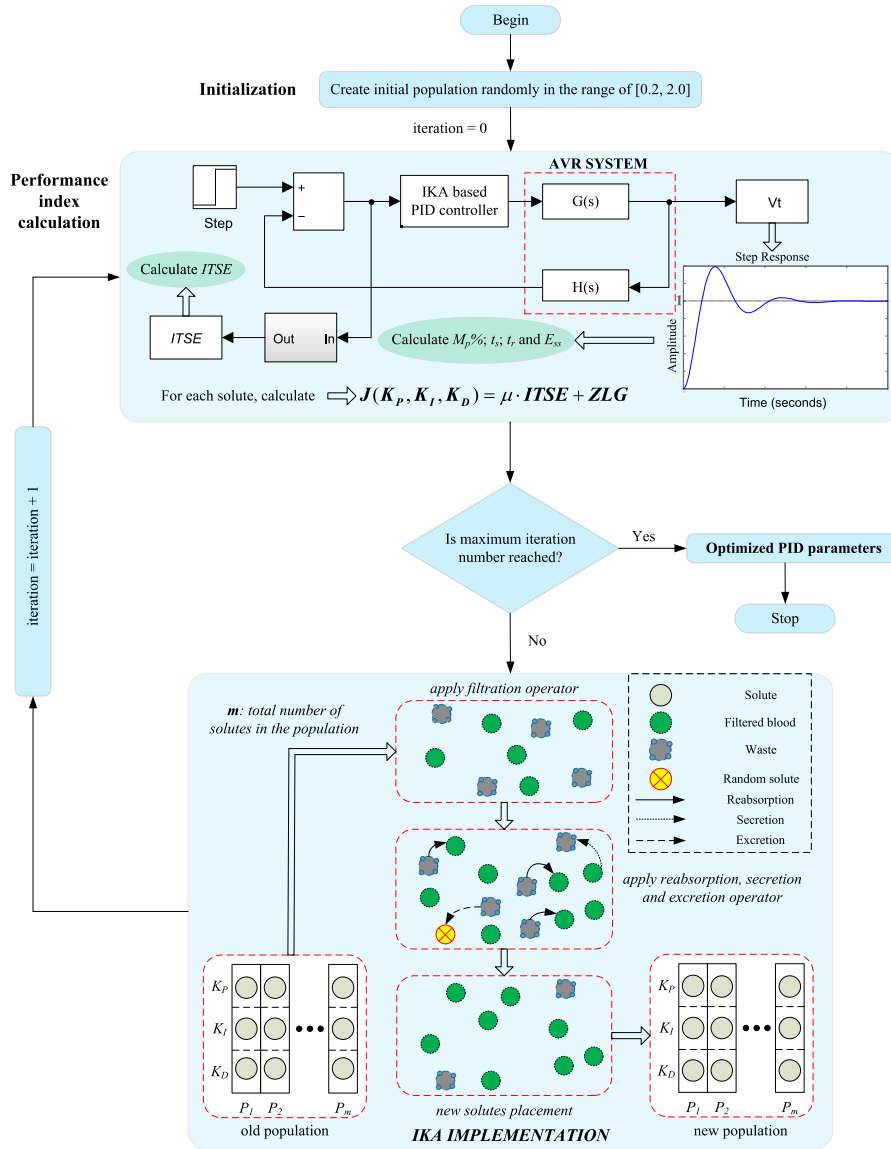


FIGURE 7. Block diagram of IKA implementation for optimizing AVR performance.

proposed IKA-PID controller.

$$\begin{aligned}
 T_{IKA-PID} &= \frac{\Delta V_t(s)}{\Delta V_{ref}(s)} \\
 &= \frac{0.05999s^3 + 6.103s^2 + 10.53s + 10.09}{0.0004s^5 + 0.0454s^4 + 0.555s^3 + 7.509s^2 + 11.43s + 10.09} \quad (16)
 \end{aligned}$$

## B. COMPARISON OF VOLTAGE RESPONSES OF AVR SYSTEM WITH DIFFERENT OPTIMIZED PID CONTROLLERS

In order to demonstrate the effectiveness and superiority of the proposed IKA-PID controller, the obtained time domain simulation responses were compared with other optimization

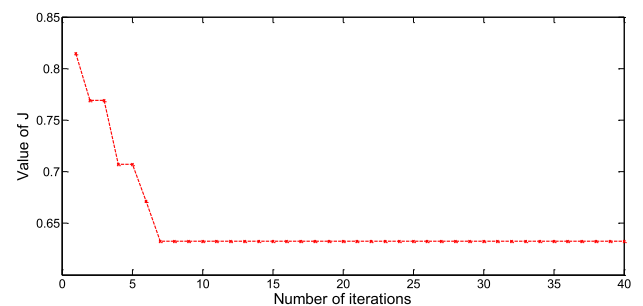


FIGURE 8. IKA-based convergence characteristics of  $J(\bar{K})$  value.

algorithms in the literature. The other algorithms that are used to design PID controller for the same AVR system are PSO [39], DE [19], ABC [19], LUS [13], PSA [18],



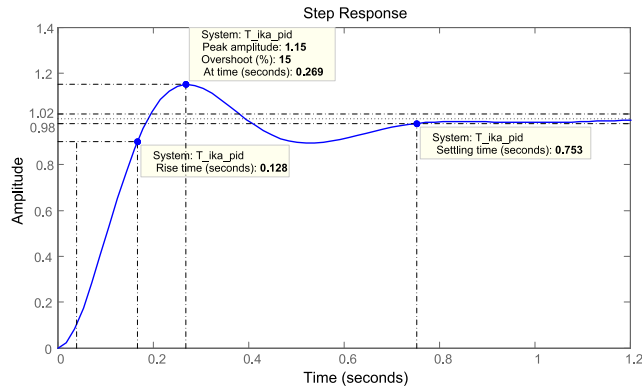


FIGURE 9. Terminal voltage step response of the AVR system with IKA-PID.

TABLE 2. Optimized PID parameters,

Controller type	PID parameters		
	$K_p$	$K_i$	$K_D$
IKA-PID (proposed)	1.0426	1.0093	0.5999
PSO-PID [39]	1.3541	0.9266	0.4378
DE-PID [19]	1.9499	0.4430	0.3427
ABC-PID [19]	1.6524	0.4083	0.3654
LUS-PID [13]	1.2012	0.9096	0.4593
PSA-PID [18]	1.2771	0.8471	0.4775
BBO-PID [8]	1.2464	0.5893	0.4596
GOA-PID [11]	1.3825	1.4608	0.5462

BBO [8] and GOA [11]. The gain parameters of the PID controller obtained with different algorithms are listed in Table 2. The comparative simulation results obtained for the terminal voltage step response of the AVR system with the different controllers are shown in Fig. 10. From the figure, it is obvious that the proposed approach gives better results than the other approaches.

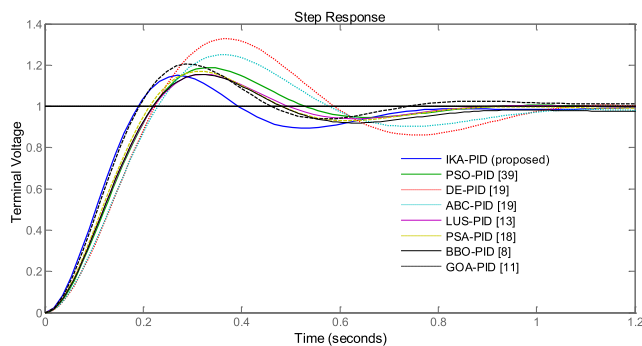


FIGURE 10. Terminal voltage changing curves of the AVR system with various controllers.

The comparative transient response analysis with performance characteristics of  $M_p\%$ ,  $t_s$ ,  $t_r$  and  $t_p$  is given in Table 3. In the table, the values of the most preferred objective functions in the optimization processes, ITSE and ZLG values, are also given for comparison purposes. As can be clearly seen from the table, the values of the four transient performance indices and the two objective functions were lowest

TABLE 3. Transient response analysis results for different controllers.

Controller type	Transient response parameters				Objective functions	
	$M_p\%$	$t_s$ (s)	$t_r$ (s)	$t_p$ (s)	ITSE	ZLG
IKA-PID (proposed)	15.00	0.753	0.128	0.269	$6.161 \times 10^{-3}$	0.3247
PSO-PID [39]	18.82	0.815	0.149	0.328	$7.172 \times 10^{-3}$	0.3640
DE-PID [19]	32.85	2.649	0.152	0.360	$2.235 \times 10^{-2}$	1.1272
ABC-PID [19]	25.01	3.094	0.156	0.360	$1.803 \times 10^{-2}$	1.2389
LUS-PID [13]	15.56	0.800	0.149	0.322	$6.408 \times 10^{-3}$	0.3381
PSA-PID [18]	16.84	0.804	0.144	0.316	$6.421 \times 10^{-3}$	0.3496
BBO-PID [8]	15.52	1.446	0.149	0.317	$7.773 \times 10^{-3}$	0.5783
GOA-PID [11]	20.53	0.971	0.130	0.286	$6.332 \times 10^{-3}$	0.4390

TABLE 4. Comparison of performance improvements in percentage contributed by IKA-based controller.

Controller type	Improvements contributed by IKA-based controller (%)					
	$M_p\%$	$t_s$	$t_r$	$t_p$	ITSE	ZLG
PSO-PID [39]	25.47	8.23	16.41	21.93	16.41	12.10
DE-PID [19]	119.00	251.79	18.75	33.83	262.77	247.15
ABC-PID [19]	66.73	310.89	21.88	33.83	192.65	281.55
LUS-PID [13]	3.73	6.24	16.41	19.70	4.01	4.13
PSA-PID [18]	12.27	6.77	12.50	17.47	4.22	7.67
BBO-PID [8]	3.47	92.03	16.41	17.84	26.16	78.10
GOA-PID [11]	36.85	28.95	1.56	6.32	2.78	35.20

with the use of the IKA-PID controller. The improvement percentages of IKA-PID for  $M_p\%$ ,  $t_s$ ,  $t_r$ ,  $t_p$ , ITSE and ZLG values are given in Table 4. As a result, the PID controller that is designed with the IKA algorithm used in conjunction with the proposed  $J(\bar{K})$  objective function for the AVR system has a more stable, faster and less oscillating structure than the other PID controllers tuned with different approaches.

### C. POLE/ZERO MAP AND BODE ANALYSES

The pole/zero map and Bode analyses were performed to evaluate the stability performance of the AVR system, which was designed with controller parameters tuned by the IKA technique. The pole/zero map and Bode plots are given in Fig. 11 and Fig. 12, respectively. The comparative simulation results obtained for AVR system are given in Table 5 and Table 6. According to the pole/zero map analysis results, the closed loop poles of the IKA-PID-based AVR system are  $s_1 = -102$ ,  $s_{2,3} = -5.13 \pm j11.7$  ve  $s_{4,5} = -0.80 \pm j0.93$ , and the corresponding damping ratios are 1.00, 0.40 and 0.65, respectively. In addition, peak gain, phase margin, delay margin and bandwidth parameters obtained from Bode analysis are 1.78 dB (10.6 rad/s), 76.7°, 0.095 s (14.0 rad/s) and 16.785, respectively. According to these results, since the closed-loop poles of the IKA-PID-based system are all in the left-half of the  $s$ -plane, the system is stable and has a very good frequency response.

### D. ROBUSTNESS ANALYSIS

Finally, the time constants of amplifier, exciter, generator and sensor were changed in steps of 25% from -50% to

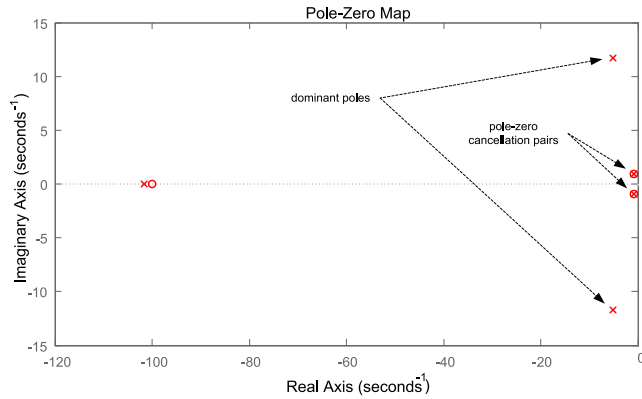


FIGURE 11. Pole-zero map of the IKA-based AVR system.

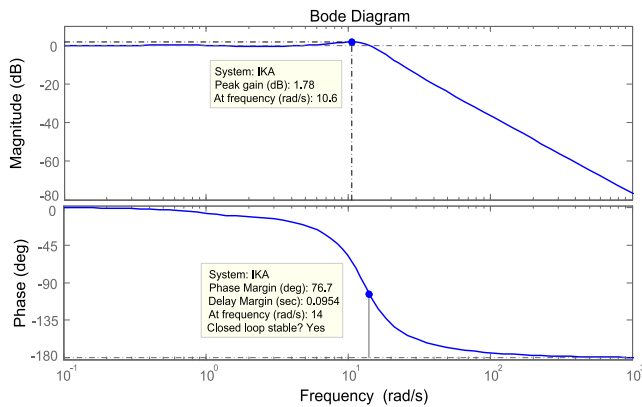


FIGURE 12. Bode analysis of the IKA-based AVR system.

+50% to examine the robustness of the AVR system with PID controller optimized by IKA technique. The results of the transient response obtained from the robustness analysis are presented in Table 7. Similarly, transient responses of the AVR system with the IKA-PID controller obtained for varying time constants are shown in Figs. 13-16. In addition, the total deviation ranges of the peak values,  $t_s$ ,  $t_r$ , and  $t_p$ , of the system examined, and the percentage of maximum deviations are shown in Table 8. The deviation ranges and percentage ratios in the table are all tolerable and these results indicate that the proposed IKA-PID-based AVR system is robust.

TABLE 6. Peak gain, phase margin, delay margin and bandwidth of AVR system.

Controller type	Peak gain	Phase margin (deg)	Delay margin	Bandwidth
IKA-PID (proposed)	<b>1.78 dB (10.6 rad/s)</b>	<b>76.7</b>	<b>0.095 s (14.0 rad/s)</b>	<b>16.785</b>
PSO-PID [39]	1.79 dB (8.29 rad/s)	79.3	0.121 s (11.5 rad/s)	13.915
DE-PID [19]	4.20 dB (7.61 rad/s)	58.4	0.092 s (11.1 rad/s)	12.800
ABC-PID [19]	2.87 dB (7.52 rad/s)	69.4	0.111 s (10.9 rad/s)	12.880
LUS-PID [13]	1.43 dB (8.59 rad/s)	83.2	0.126 s (11.6 rad/s)	14.208
PSA-PID [18]	1.68 dB (8.89 rad/s)	79.7	0.115 s (12.1 rad/s)	14.636
BBO-PID [8]	1.56 dB (8.65 rad/s)	81.6	0.122 s (11.7 rad/s)	14.284
GOA-PID [11]	2.13 dB (9.81 rad/s)	73.4	0.095 s (13.4 rad/s)	15.958

TABLE 5. Closed loop poles and damping ratios of AVR system.

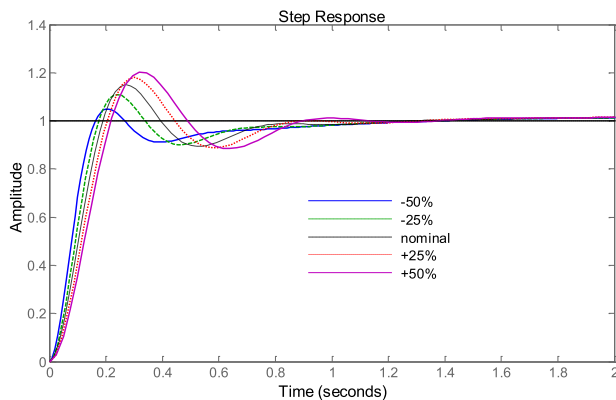
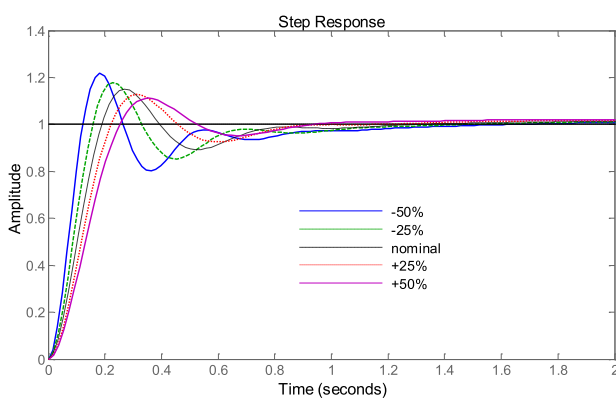
Controller type	Closed loop poles	Damping ratio
IKA-PID (proposed)	-102	1.00
	-5.13 + j11.7	0.40
	-5.13 - j11.7	0.40
	-0.80 + j0.93	0.65
	-0.80 - j0.93	0.65
PSO-PID [39]	-102	1.00
	-1.02	1.00
	-2.00	1.00
	-4.64 + j9.50	0.439
	-4.64 - j9.50	0.439
DE-PID [19]	-100.91	1.00
	-3.02 + j8.19	0.34
	-3.02 - j8.19	0.34
	-6.29	1.00
	-0.22	1.00
ABC-PID [19]	-100.98	1.00
	-3.75 + j8.40	0.40
	-3.75 - j8.40	0.40
	-4.74	1.00
	-0.25	1.00
LUS-PID [13]	-101	1.00
	-1.24 + j0.56	0.91
	-1.24 - j0.56	0.91
	-4.88 + j9.88	0.44
	-4.88 - j9.88	0.44
PSA-PID [18]	-101	1.00
	-1.28 + j0.15	0.99
	-1.28 - j0.15	0.99
	-4.82 + j10.1	0.43
	-4.82 - j10.1	0.43
BBO-PID [8]	-100.00	1.00
	-4.80 + j10.2	0.427
	-4.80 - j10.2	0.427
	-2.1	1.00
	-0.585	1.00
GOA-PID [11]	-101	1.00
	-1.18 + j1.06	0.74
	-1.18 - j1.06	0.74
	-4.83 + j10.9	0.40
	-4.83 - j10.9	0.40

## E. SIMULINK IMPLEMENTATION

In order to get the controller efforts, since MATLAB Simulink implementation requires a non-ideal transfer function for the used controller, the proposed IKA-based PID controller realized with a first-order filter on derivative term and

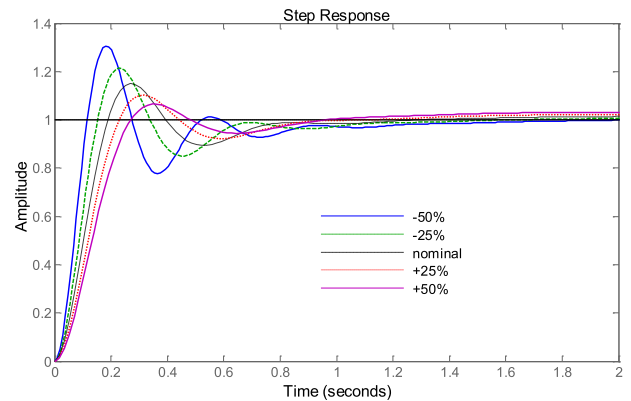
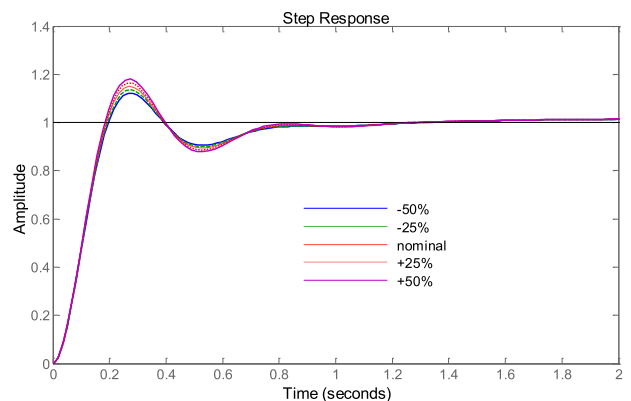
**TABLE 7. Results of robustness analysis of the control system optimized with IKA technique.**

Model Parameters	Rate of change (%)	Peak value (p.u.)	$t_s$ (s)	$t_r$ (s)	$t_p$ (s)
$T_A$	-50	1.049	0.965	0.107	0.211
	-25	1.109	0.967	0.118	0.241
	+25	1.180	0.795	0.138	0.299
	+50	1.203	0.845	0.147	0.319
$T_E$	-50	1.218	1.167	0.084	0.182
	-25	1.179	1.041	0.106	0.227
	+25	1.128	0.804	0.150	0.310
	+50	1.111	2.105	0.170	0.351
$T_G$	-50	1.306	1.236	0.078	0.182
	-25	1.214	1.052	0.103	0.230
	+25	1.102	2.449	0.153	0.318
	+50	1.065	2.826	0.179	0.349
$T_S$	-50	1.121	0.786	0.133	0.282
	-25	1.136	0.768	0.130	0.276
	+25	1.164	0.742	0.126	0.263
	+50	1.180	0.733	0.124	0.275

**FIGURE 13. Voltage change curves for  $T_A$  varying from -50% to +50%.****FIGURE 14. Voltage change curves for  $T_E$  varying from -50% to +50%.**

then its implementation are tested in Simulink. The transfer function of the PID controller using a first-order filter is given as follows:

$$G_{PID\_filter} = K_P + \frac{K_I}{s} + \frac{sK_D}{T_f s + 1} \quad (17)$$

**FIGURE 15. Voltage change curves for  $T_G$  varying from -50% to +50%.****FIGURE 16. Voltage change curves for  $T_S$  varying from -50% to +50%.****TABLE 8. Range of total deviations and percentage of maximum deviations of the system.**

Model parameters	Performance parameters	Range of total deviation	Percentage of maximum deviation (%)
$T_A$	Peak value (p.u.)	0.154	8.78
	$t_s$ (s)	0.172	28.42
	$t_r$ (s)	0.040	16.41
	$t_p$ (s)	0.108	21.56
$T_E$	Peak value (p.u.)	0.107	5.91
	$t_s$ (s)	1.301	179.55
	$t_r$ (s)	0.086	34.37
	$t_p$ (s)	0.169	32.34
$T_G$	Peak value (p.u.)	0.241	13.57
	$t_s$ (s)	1.774	275.29
	$t_r$ (s)	0.101	39.84
	$t_p$ (s)	0.167	32.34
$T_S$	Peak value (p.u.)	0.059	2.61
	$t_s$ (s)	0.053	4.38
	$t_r$ (s)	0.009	3.91
	$t_p$ (s)	0.019	4.83

where  $T_f$  is the time constant of the first-order filter that is set to 0.001 [6]. Comparative performance of the controller outputs tuned by various approaches in terms of the controller efforts is given in Table 9.

**TABLE 9.** Energy and maximum control signal of controllers.

Controller type	Energy	$U_{\max}$
IKA-PID (proposed)	190.6099	600.9426
PSO-PID [39]	101.7378	439.1541
DE-PID [19]	63.1750	344.6499
ABC-PID [19]	<b>71.3077</b>	<b>367.0524</b>
LUS-PID [13]	111.7809	460.5012
PSA-PID [18]	120.9099	478.7771
BBO-PID [8]	111.9957	460.8464
GOA-PID [11]	158.3456	547.5825

From the table, it is seen that the controller with the highest control effort is the proposed IKA-based PID controller. In fact, although it seems to give the worst results, these results are perfectly normal since the proposed controller is the fastest responding controller according to the values given in Table 3. That is the controller is exerting more effort for a faster transient response. The ABC algorithm, which is the least effort consuming controller, gives the slowest transient response in Table 3 and confirms the results we obtained.

## VI. CONCLUSION

In this study, IKA technique, which is an improved version of the original KA technique that is inspired by the basic function of the kidneys in the human body, has been proposed for the first time in PID controller design in AVR system. The improved algorithm is a self-adaptive algorithm with advanced convergence capabilities. During the parameter tuning process, the IKA technique was run several times through a proposed novel objective function that accommodates the advantages of the two most common used objective functions with minimum number of iterations and the optimal values of PID gains were found. In order to reveal the usefulness of the presented design, the performance comparisons are done with seven different optimization algorithms (PSO [39], DE [19], ABC [19], LUS [13], PSA [18], BBO [8] and GOA [11]) that have been published in recent years in literature. The simulation results showed that the system controller tuned by IKA technique had a better transient response profile compared to the other available techniques in terms of  $M_p\%$ ,  $t_s$ ,  $t_r$  and  $t_p$  values. Thus, the values of the ITSE and ZLG objective functions have also been successfully reduced. In addition, pole/zero map analysis, Bode analysis and robustness analysis were performed to evaluate the stability of the system tuned by IKA technique. From these analyses, it was found that the system had a good stability structure and the proposed IKA-PID controller was not affected by the changes in system parameters.

## REFERENCES

- [1] S. Chatterjee and V. Mukherjee, "PID controller for automatic voltage regulator using teaching-learning based optimization technique," *Int. J. Elect. Power Energy Syst.*, vol. 77, pp. 418–429, May 2016.
- [2] B. Hekimoğlu, S. Ekinici, V. Demiray, R. Doguruci, and A. Yıldırım, "Speed control of DC motor using PID controller tuned by salp swarm algorithm," in *Proc. IENSC*, Diyarbakır, Turkey, 2018, pp. 1878–1889.
- [3] K. Ogata, *Modern Control Engineering*, 4th ed. Upper Saddle River, NJ, USA: Prentice-Hall, 2002.
- [4] B. Hekimoğlu, S. Ekinici, and S. Kaya, "Optimal PID controller design of DC-DC buck converter using whale optimization algorithm," in *Proc. IEEE IDAP*, Malatya, Turkey, Sep. 2018, pp. 473–478.
- [5] A. Rubaai and P. Young, "EKF-based PI-/PD-like fuzzy-neural-network controller for brushless drives," *IEEE Trans. Ind. Appl.*, vol. 47, no. 6, pp. 2391–2401, Nov./Dec. 2011.
- [6] Z. Bingul and O. Karahan, "A novel performance criterion approach to optimum design of PID controller using cuckoo search algorithm for AVR system," *J. Franklin Inst.*, vol. 355, no. 13, pp. 5534–5559, 2018.
- [7] F. Olivas, L. Amador-Angulo, J. Perez, C. Caraveo, F. Valdez, and O. Castillo, "Comparative study of type-2 fuzzy particle swarm, bee colony and bat algorithms in optimization of fuzzy controllers," *Algorithms*, vol. 10, no. 3, p. 101, 2017.
- [8] U. Güvenç, T. Yiğit, A. H. I. ik, and I. Akkaya, "Performance analysis of biogeography-based optimization for automatic voltage regulator system," *Turkish J. Elect. Eng. Comput. Sci.*, vol. 24, no. 3, pp. 1150–1162, 2016.
- [9] S. Duman, N. Yörüken, and I. H. Alta, "Gravitational search algorithm for determining controller parameters in an automatic voltage regulator system," *Turkish J. Elect. Eng. Comput. Sci.*, vol. 24, no. 4, pp. 2387–2400, 2016.
- [10] A. Kumar and G. Shankar, "Priority based optimization of PID controller for automatic voltage regulator system using gravitational search algorithm," in *Proc. IEEE RDCAPE*, Noida, India, Mar. 2015, pp. 292–297.
- [11] B. Hekimoğlu and S. Ekinici, "Grasshopper optimization algorithm for automatic voltage regulator system," in *Proc. IEEE 5th ICEEE*, Istanbul, Turkey, May 2018, pp. 152–156.
- [12] O. Bendjeghaba, "Continuous firefly algorithm for optimal tuning of PID controller in AVR system," *J. Elect. Eng.*, vol. 65, no. 1, pp. 44–49, 2014.
- [13] P. K. Mohanty, B. K. Sahu, and S. Panda, "Tuning and assessment of proportional-integral-derivative controller for an automatic voltage regulator system employing local unimodal sampling algorithm," *Electr. Power Compon. Syst.*, vol. 42, no. 9, pp. 959–969, 2014.
- [14] S. Priyambada, P. K. Mohanty, and B. K. Sahu, "Automatic voltage regulator using TLBO algorithm optimized PID controller," in *Proc. IEEE 9th ICIS*, Gwalior, India, Dec. 2014, pp. 1–6.
- [15] H. M. Hasanien, "Design optimization of PID controller in automatic voltage regulator system using Taguchi combined genetic algorithm method," *IEEE Syst. J.*, vol. 7, no. 4, pp. 825–831, Dec. 2013.
- [16] S. Panda, B. K. Sahu, and P. K. Mohanty, "Design and performance analysis of PID controller for an automatic voltage regulator system using simplified particle swarm optimization," *J. Franklin Inst.*, vol. 349, no. 8, pp. 2609–2625, 2012.
- [17] H. Shayeghi and J. Dadashpour, "Anarchic society optimization based PID control of an automatic voltage regulator (AVR) system," *Elect. Electron. Eng.*, vol. 2, no. 4, pp. 199–207, 2012.
- [18] B. K. Sahu, P. K. Mohanty, S. Panda, and N. Mishra, "Robust analysis and design of PID controlled AVR system using pattern search algorithm," in *Proc. IEEE PEDES*, Bengaluru, India, Dec. 2012, pp. 1–6.
- [19] H. Gozde and M. C. Taplamacioglu, "Comparative performance analysis of artificial bee colony algorithm for automatic voltage regulator (AVR) system," *J. Franklin Inst.*, vol. 348, no. 8, pp. 1927–1946, 2011.
- [20] L. dos Santos Coelho, "Tuning of PID controller for an automatic voltage system using chaotic optimization approach," *Chaos, Soliton Fractals*, vol. 39, no. 4, pp. 1504–1514, 2009.
- [21] H. Zhu, L. Li, Y. Zhao, Y. Guo, and Y. Yang, "CAS algorithm-based optimum design of PID controller in AVR system," *Chaos, Soliton Fractals*, vol. 42, no. 2, pp. 792–800, 2009.
- [22] Z.-L. Gaing, "A particle swarm optimization approach for optimum design of PID controller in AVR system," *IEEE Trans. Energy Convers.*, vol. 19, no. 2, pp. 384–391, Jun. 2004.
- [23] E. Çelik, "Incorporation of stochastic fractal search algorithm into efficient design of PID controller for an automatic voltage regulator," *Neural Comput. Appl.*, vol. 30, no. 6, pp. 1991–2002, 2018.
- [24] E. Çelik and R. Durgut, "Performance enhancement of automatic voltage regulator by modified cost function and symbiotic organisms search algorithm," *Eng. Sci. Technol. Int. J.*, vol. 21, pp. 1104–1111, Oct. 2018.
- [25] S. Anbarasi and S. Muralidharan, "Enhancing the transient performances and stability of AVR system with BFOA tuned PID controller," *J. Control Eng. Appl. Inf.*, vol. 18, no. 1, pp. 20–29, 2016.
- [26] R. Pradhan, S. K. Majhi, and B. P. Pati, "Design of PID controller for automatic voltage regulator system using Ant Lion Optimizer," *World J. Eng.*, vol. 15, no. 3, pp. 373–387, 2017.

- [27] B. Hekimoğlu, "Sine-cosine algorithm-based optimization for automatic voltage regulator system," *Trans. Inst. Meas. Control*, vol. 41, no. 6, pp. 1761–1771, 2019.
- [28] S. Ekinci, B. Hekimoğlu, and S. Kaya, "Tuning of PID controller for AVR system using salp swarm algorithm," in *Proc. IEEE IDAP*, Malatya, Turkey, Sep. 2018, pp. 424–429.
- [29] N. Razmjoo, M. Khalilpour, and M. Ramezani, "A new meta-heuristic optimization algorithm inspired by FIFA world cup competitions: Theory and its application in PID designing for AVR system," *J. Control, Automat. Elect. Syst.*, vol. 27, no. 4, pp. 419–440, 2016.
- [30] D. K. Sambariya and T. Gupta, "Optimal design of PID controller for an AVR system using monarch butterfly optimization," in *Proc. IEEE ICICIC*, Indore, India, Aug. 2017, pp. 1–6.
- [31] S. Ekinci, A. Demiroren, and B. Hekimoğlu, "Parameter optimization of power system stabilizers via kidney-inspired algorithm," *Trans. Inst. Meas. Control*, vol. 41, no. 5, pp. 1405–1417, 2019.
- [32] N. N. Islam, M. A. Hannan, H. Shareef, and A. Mohamed, "An application of backtracking search algorithm in designing power system stabilizers for large multi-machine system," *Neurocomputing*, vol. 237, pp. 175–184, May 2017.
- [33] N. S. Jaddi, J. Alvankarian, and S. Abdullah, "Kidney-inspired algorithm for optimization problems," *Commun. Nonlinear Sci. Numer. Simul.*, vol. 42, pp. 358–369, Jan. 2017.
- [34] M. Ehteram, H. Karami, S. F. Mousavi, S. Farzin, A. B. Celeste, and A.-E. Shafie, "Reservoir operation by a new evolutionary algorithm: Kidney algorithm," *Water Resour. Manage.*, vol. 32, no. 14, pp. 4681–4706, 2018.
- [35] S. Ekinci, B. Hekimoğlu, and E. Uysal, "Kidney-inspired algorithm for determination of PID power system stabilizer parameters," *J. Polytech.*, vol. 22, no. 2, pp. 453–460, 2019. doi: [10.2339/politeknik.417765](https://doi.org/10.2339/politeknik.417765).
- [36] Y. Liang, D. Niu, H. Wang, and H. Chen, "Assessment analysis and forecasting for security early warning of energy consumption carbon emissions in Hebei Province, China," *Energies*, vol. 10, no. 3, p. 391, 2017.
- [37] M. Du, D. Zhao, B. Yang, and L. Wang, "Terminal sliding mode control for full vehicle active suspension systems," *J. Mech. Sci. Technol.*, vol. 32, no. 6, pp. 2851–2866, 2018.
- [38] N. S. Jaddi and S. Abdullah, "Optimization of neural network using kidney-inspired algorithm with control of filtration rate and chaotic map for real-world rainfall forecasting," *Eng. Appl. Artif. Intell.*, vol. 62, pp. 246–259, Jan. 2018.
- [39] M. A. Sahib, "A novel optimal PID plus second order derivative controller for AVR system," *Eng. Sci. Technol. Int. J.*, vol. 18, no. 2, pp. 194–206, 2015.
- [40] H. Saadat, *Power System Analysis*. New York, NY, USA: McGraw-Hill, 1999.
- [41] J. E. Hall, *Guyton and Hall Textbook of Medical Physiology*. Philadelphia, PA, USA: Elsevier, 2015.
- [42] A. Sikander, P. Thakur, R. C. Bansal, and S. Rajasekar, "A novel technique to design cuckoo search based FOPID controller for AVR in power systems," *Comput. Elect. Eng.*, vol. 70, pp. 261–274, Aug. 2018.



**SERDAR EKİNCİ** was born in Diyarbakir, Turkey, in 1984. He received the B.S. degree in control engineering, and the M.S. and Ph.D. degrees in electrical engineering from Istanbul Technical University (ITU), in 2007, 2010, and 2015, respectively.

Since 2016, he has been an Assistant Professor with the Computer Engineering Department, Batman University, Batman, Turkey. His areas of interests are electrical power systems, stability, control technology, and the applications of heuristic optimization to power system control.



**BARAN HEKİMOĞLU** (M'00) was born in Diyarbakir, Turkey, in 1974. He received the B.S. degree in electrical engineering from Istanbul Technical University, Istanbul, Turkey, in 1997, the M.S. degree in mathematics education from Florida State University, Tallahassee, FL, USA, in 2001, and the Ph.D. degree in electrical engineering from Kocaeli University, Kocaeli, Turkey, in 2010.

He was a Research Assistant (2003–2011), and was also an Assistant Professor (2011–2013) with the Civil Aviation School, Kocaeli University. Since 2013, he has been an Assistant Professor with the Electrical and Electronics Engineering Department, Batman University, Batman, Turkey. His research interests include power electronics and power systems control.

Dr. Hekimo lu has been a member of the Chamber of Electrical Engineers (EMO), Turkey, since 1997.

• • •